

A review on Radiation Detectors for Various Radiation Detection Applications

Arpit Patel^{1,2*} and Himanshu Mazumdar²

¹ Physical Research Laboratory, Ahmedabad 380009, Gujarat, India

² Research and development department, Dharamsinh Desai university, Nadiad 387001, Gujarat, India.

Received: 28 Feb. 2023, Revised: 12 Mar. 2023, Accepted: 22 Mar. 2023.

Published online: 1 May 2023.

Abstract: This paper provides a review of radiation detectors to measure the ionizing radiation like gamma-ray, X-ray, high energy UV-ray and heavy ions, etc. It is essential to know about the radiation source and its effects for several applications such as aviation, medical, high energy physics experiments and space missions. In the last few decades, numerous detectors with different manufacturing technologies have been reported. Semiconductor devices such as diodes, metal-oxide-semiconductor field-effect transistors (MOSFETs) and solid-state photomultipliers (SSPMs), etc., have been made and widely used to measure different kind of radiation. This article goes through the evolution of radiation detectors design using various technologies and summarizes the features with emphasis on their underlying principles and applications.

Keywords: Radiation detector, Silicon drift detector, SiPM, Scintillator, Gamma ray detector, X-ray, Spectrometer.

1 Introduction

Radiation is a form of energy that is emitted or transmitted in the form of rays, electromagnetic waves, and/or particles. In some cases, radiation can be seen (visible light) or felt (infrared radiation), while other forms like X-rays and gamma rays are not visible and can only be observed directly or indirectly with special equipment. Radiation can be described as being one of two basic types: non ionizing and ionizing.

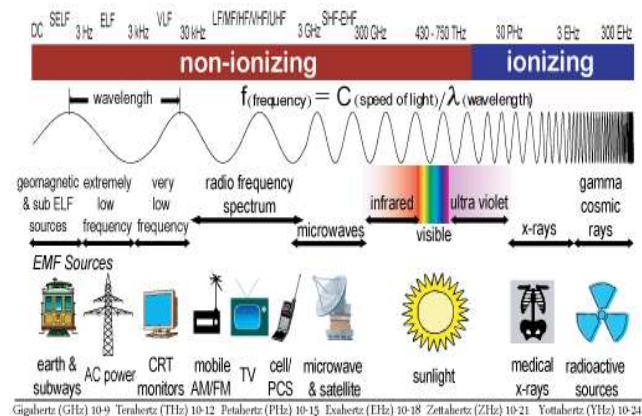


Fig. 1: Types of radiation on the electromagnetic spectrum [1].

1.1 Non-ionizing radiation

Each day, people are exposed to non-ionizing radiation sources. In this form of radiation, there is not enough energy to cause atoms or molecules to ionize. It is common for microwave ovens, global positioning systems, cellular telephones, television stations, FM and AM radios, baby monitors, cordless phones, garage-door openers, and ham radios to emit non-ionizing radiation. In addition to the earth's magnetic field, electromagnetic field exposure from electrical appliances, household wiring, and transmission lines can also be caused by magnetic field exposure. These waves are defined as extremely low frequency (ELF) waves.

1.2 Ionizing radiation

A certain type of radiation has enough energy to knock electrons out of their orbits around an atom, upsetting the electron/proton balance and giving the atom a positive charge. Atoms and molecules that are electrically charged are called ions [2]. Radiation that can produce ions is referred to as ionizing radiation.

Several types of ionizing radiation exist, mainly due to charged particles, neutral particles, and photons. The following are some of the relevant ones:

*Corresponding author e-mail: arpit_0046@yahoo.com

1.2.1 Alpha radiation:

As alpha radiation is composed of two protons and two neutrons without an electron, they carry a positive charge. Alpha particles are not able to penetrate skin due to their size and charge, and can be stopped completely by a sheet of paper [3].

1.2.2 Beta radiation:

Atoms eject fast-moving electrons from their nuclei generate beta radiation. Compared with alpha particles, beta radiation has a negative charge and is about 1/7000th the size [3], which makes it more penetrating than alpha. A small amount of shielding, such as a plastic sheet, can still block it.

1.2.3 Gamma radiation:

In the case of gamma radiation, the penetration is very great. Usually, it is released immediately after an alpha or beta particle is emitted from an atom's nucleus. Due to its lack of mass or charge, it can pass through the human body, but denser materials, such as concrete or lead, absorb it [3].

1.2.4 X-rays:

Like gamma radiation, X-rays are produced primarily artificially rather than from radioactive substances [3].

1.2.5 Neutron radiation:

Nuclear fission and other processes eject neutrons from the nucleus, causing neutron radiation. A nuclear chain reaction occurs when a neutron is ejected from one fissioned atom, causing another to fission, releasing more neutrons. In contrast to other radiations, neutron radiation is absorbed by materials that contain a lot of hydrogen atoms, such as paraffin wax and plastics. The types of decay for various radiations are shown in Figure 2.

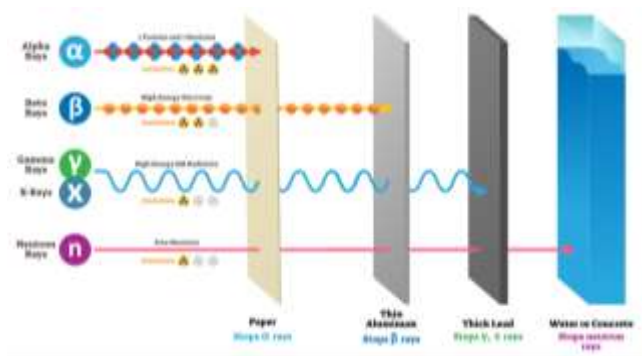


Fig. 2. Types of decay for various radiation [2].

Throughout daily lives, people are constantly exposed to electromagnetic radiation via the use of

microwaves, cell phones, and diagnostic medical imaging. There are many naturally occurring sources of electromagnetic and ionizing radiation. These include radioactive elements in the Earth's crust, radiation trapped in the Earth's magnetic field, stars, and other astrophysical objects like quasars or galactic centers [2]. Also, Human-created technologies emits electromagnetic radiation like radio transmitters, light bulbs, heaters, and gamma-ray sterilizers etc. Earth's biggest source of radiation is the Sun. All electromagnetic spectrum wavelengths are emitted by the Sun. The most prevalent types of radiation are visible, infrared, and ultraviolet radiation (UV). Solar flares and coronal mass ejections (CMEs), which are enormous explosions that occasionally take place on the surface of the Sun, unleash enormous quantities of energy into space in the form of x-rays, gamma rays, and streams of protons and electrons known as solar particle events (SPE). GCR, also known as galactic cosmic radiation, is a type of radiation that originates largely from within our Milky Way galaxy but also from sources outside the solar system. As they travelled through the galaxy at almost the speed of light, GCR are hefty, high-energy ions of elements that have had all of their electrons stripped away. They can ionize atoms as they move through matter and can almost completely pass through an astronaut's skin or a standard spaceship. In our solar system, the GCRs are a significant source of radiation that must be managed on board both existing and future spacecraft [2]. The average intensity of these particles is at its peak when there are the fewest sunspots because they are influenced by the Sun's magnetic field.

2 Radiation sensors review

For monitoring, measuring, and control systems, a sensor is a device or component of a system that is used to measure physical, chemical, biological, and any other factors [4]. Radiation is described as the energy emitted from a source through a medium in the form of waves and particles, from radio waves, which have the smallest wavelengths, to gamma radiation, which has the highest energies in the electromagnetic spectrum.

Based on the idea of ionization, a radiation detector is a special device that is used to find nuclear particles including alpha, beta, gamma, X-ray, and proton [5]. When a highly energetic nuclear particle interacts with a material medium, it ionizes the substance, which allows the radiation to be detected using a variety of sensor techniques. Depending on the type of detector being used, the conversion factor used to turn the photon energy emitted during the collision into an electrical signal might be either direct or indirect [6]. Hence, the radiation detectors are broadly classified in to two types

1. Direct conversion type
2. Indirect conversion type

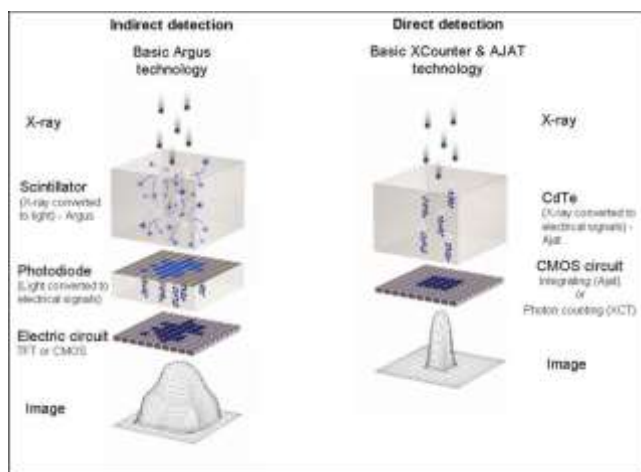


Fig.3. Schematic representation of production of charge carriers in direct and indirect conversion type X-ray detectors [7].

A direct conversion type detector is the one in which the incoming photon is directly converted into an electrical signal, whereas in an indirect conversion type detector, the conversion takes place in two steps. The first step involves conversion of a photon into visible light, and the second step involves the conversion of visible light into an electrical pulse. The schematic representation of production of charge carriers in direct and indirect conversion type detectors is shown in **Error! Reference source not found.3**.

The indirect conversion approach induces loss of information in the process, particularly at very low radiation inputs. The incident photon energy is directly transformed into a certain amount of charge that is subsequently collected at the device's output electrode in the case of semiconductor and gas-filled detectors. In direct conversion type, there is no charge loss, and hence provides good energy resolution. The energy required to create one electron-hole (e-h) pair in gas-filled detectors varies from 25 - 35 eV, and in the case of a semiconductor detector, it is of the order of a few eVs (for silicon, 3.6 eV and for germanium, 2.9 eV). Scintillation detectors are indirect conversion type, where the incident radiation is converted into a shower of optical photons (visible and near visible region). These photons are then collected and converted into electrical charge by using photo detectors. The photo detector could be a photomultiplier tube (PMT) or a silicon photo detector or a very recent technology device known as silicon photomultipliers (SPM). Due to the two-step conversion mechanism in the indirect conversion process, there is a loss of signal due to light coupling, resulting in poor energy resolution. The average energy required to create one e-h pair in scintillators is of the order of 25 eV.

When a highly energetic nuclear particle enters a material medium, it ionizes the medium, and, through different sensor mechanisms, the radiation can be detected. The detection of such energy requires different types of

sensors, broadly classified in Figure 4.

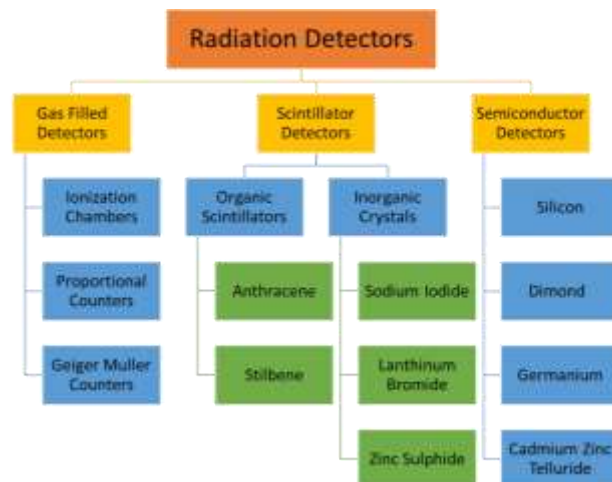


Fig. 4. The classification of radiation detectors that are being used in radiation monitoring.

The aim of upcoming sections is to introduce various types of detectors used in X-ray, Gamma-ray and particle detection, with emphasis on semiconductor detectors and, in particular, the silicon detectors. An X-ray or gamma-ray detector is a transducer which converts the photon energy into voltage pulses. The interaction of an X-ray photon within the active volume of the detector produces charge carriers (electron-hole pairs) through the photoionization process. The current pulse produced by these charge carriers is converted to a voltage pulse by a charge-to-voltage conversion amplifier known as a charge-sensitive pre-amplifier. The voltage amplitude of the pulse is proportional to the energy of the incident X-ray photon. The signal is then processed by a suitable low-noise electronics chain to obtain the energy and other required parameters such as arrival time, angle of arrival, position of interaction, etc. X-ray detectors are also used to detect other types of electromagnetic radiations such as electrons, protons, and alphas, etc.

2.1 Gas-filled detectors

In comparison to a scintillator detector or a semiconductor detector, the gas-filled detector is the most straightforward. An electrode filled with inert gas serves as the medium in this type of detector, which is housed in a metallic or plastic cylinder made of another material, such as plastic. The electrode is connected to a pure capacitive load or an electrical circuit that includes a power source, a load resistor, and a signal. When ionizing radiation is incidentally introduced into the medium, it ionizes the inert gas and generates ion-free electron pairs that are subsequently exposed to an electric field. The free electron goes toward the electrode and into the electric circuit as the positive ion advances towards the surface of the cylinder, producing an electric pulse or count before it returns to the metallic cylinder and recombines with the positive ion and

becomes neutral again. Gas-Filled Detectors come in three different varieties: ionization chambers, proportional counters, and Geiger-Muller counters.

2.1.1 Ionization Chamber

The simplest type of gas-filled detector is an ionization chamber, which use the Bragg-Gray principle to measure the rate of X-ray and gamma radiation exposure as well as the dose received [10]. It operates at a low voltage and doesn't cause an avalanche of electrons or have a dead time problem. With the use of a tiny glass, an ionization chamber can detect alpha and beta particles [11]. Ionization chambers are used for a variety of purposes, including radiation survey devices [12], a radiation source calibrator, and ionization remote sensing [5].

2.1.2 The Proportional Counter

The concept of proportional counter was introduced in the late 1940's. Proportional counter is gas filled device, used as X-ray detector with moderate energy resolution by operating at room temperature [13]. Proportional counters are generally made in cylindrical form and the internal volume is filled with gas as shown in Figure 5. The most widely utilized gases are krypton, xenon, neon, and high purity argon. A wire running along the cylinder's axis serves as the anode, and the surface outside the cylinder serves as the cathode. The anode has a favorable tilt toward the cathode. These detectors are generally made in large detection area with high count rate capability. The working principle of the proportional counter is that, the electrons produced by X-ray photon in the gas which is mainly due to photoelectric effect are accelerated towards the anode by applying suitable voltage across the electrodes and thus producing ionization by their collision with the atoms of the gas.

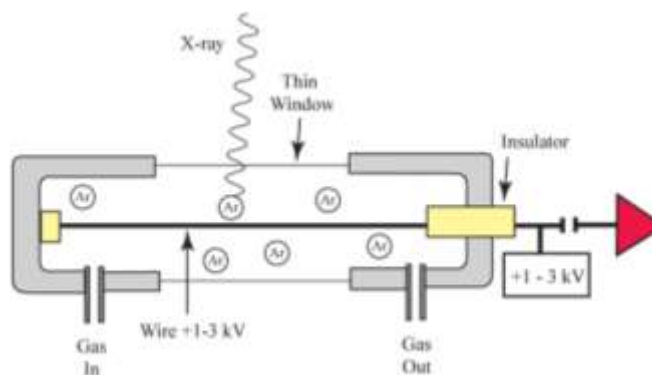


Fig. 5. Schematic representation of a cylindrical proportional counter [14].

Depending on the voltage used, the multiplication factor's value could range between 10 and 10^4 . Proportional counters typically have a diameter of 2 to 5 cm. The efficiency of these detectors in low and medium X-ray

energies is small compared to other detectors discussed in the subsequent sections. For example, 5 cm thick proportional counter filled with Ar gives 50% transmission at 10 keV and for Xe gas, the same transmission could be achieved at 40 keV at room temperature. The energy resolution of these detectors is poorer than semiconductor detectors and better than scintillator detectors. At 5.9 keV, a gas proportional has an energy resolution of between 10 and 15 percent.

2.1.3 Geiger-Muller Detector

The Geiger-Muller (GM) tube uses the same Townsend avalanche-inducing mechanism as a proportional counter, but the gas amplification brought on by a single avalanche is greater, on the order of 10^6 – 10^8 [5]. There is an uncontrollable chain avalanche that spreads across the full volume of gas in the cylinder as a result of the de-excitation of secondary free electrons, which releases an ultraviolet photon with enough energy to start another avalanche from the gas or even the tube wall. The time it takes to complete this process is between 200 and 400 seconds. The Geiger-Muller detector is thought to be dead at this point and unable to detect any further nuclear particles. If alcohol is added within the gaseous tube, such as 10% ethanol, the extra energy in the form of vibrational and rotational energy may be absorbed. As a result, it helps to shorten the period of time the counter is idle before it can start counting again. The Geiger-Muller counter cannot distinguish the energy of the incident particles based on the pulse size for selective energy counting since a low energetic particle can create an avalanche across the entire chamber [15]. To detect the presence of charged particles, neutrons, and photons, the Geiger-Muller counter is a trustworthy detector [16].

2.2 Scintillation detectors

The scintillation detector is a type of luminescent material which produces scintillation light on photon interaction. The process of fluorescence is the prompt emission of visible light from the material following its excitation by some means. Small amounts of impurities are generally added to all scintillators to enhance the emission of visible light photons. The schematic representation of scintillator working principle is shown in Figure 6.

Scintillation detectors are broadly classified into two types based on the scintillation mechanism [5], they are

1. Organic scintillators
2. Inorganic scintillators

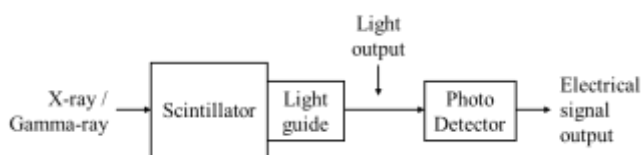


Fig. 6. Schematic representation of working principle of scintillation detector.

In case of organic scintillators, the fluorescence process arises from the transition in the energy level structure of a single molecule and therefore can be observed from a given molecular species independent of its physical state. Some examples of the organic scintillators are plastic scintillators, pure organic crystals and liquid organic crystals. These scintillators are generally used for timing applications.

In case of inorganic scintillators, the scintillation mechanism depends on the structure of the crystal lattice. In a pure inorganic crystal such as NaI, the electrons are only allowed to occupy selected energy bands. The absorption of incident photon energy in pure crystals can elevate the electrons from the valence band to the conduction band leaving gap in the valence band. The return of an electron with the emission of a photon is an inefficient process, only few photons are released by decay and the energy is released by some other mechanisms. Also, the bandgap in the pure crystals are such that the emitted photon energy is too high to lie in the visible range and therefore, some small amounts of impurities are added to the crystal in trace amounts. These impurities are called activators and they create special sites in the lattice which modifies the bandgap structure at that site. The energy structure of the overall crystal remains unchanged. Some of the inorganic scintillators are Sodium Iodide (NaI(Tl)), Cesium Iodide (CsI(Tl)), Bismuth Germanate (BGO) and Lanthanum Bromide (LaBr₃(Ce)) [5]. Inorganic scintillators are generally used for spectroscopy.

Ideal scintillators material should have the following properties

1. High scintillation efficiency.
2. Linear conversion - light yield proportional to the deposited energy for wide energy range.
3. Transparent medium for good light collection.
4. Short decay time for fast signal pulses.
5. Good optical quality with refractive index near to that of glass (~1.5).

The scintillation detectors are based on higher Z material with higher density than the gas detectors. These detectors are frequently offered in thicker versions. These elements increase the likelihood that scintillation detectors will find

photons throughout a larger energy range. These detectors' energy resolution, which ranges from 20 to 30 percent at 5.9 keV, is lower in the low energy X-ray domain. Figure 7 shows a schematic illustration of a scintillator linked with a Photo Multiplier Tube (PMT) for charge readout.

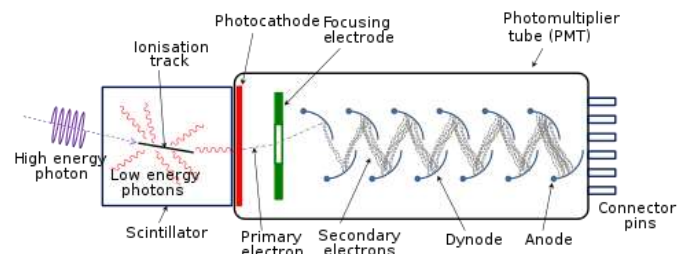


Fig. 7. Schematic representation scintillator coupled with PMT for charge readout [17].

These detectors are frequently employed in low-resolution applications where a large surface area covering a broad energy range, ranging from a few tens of keV to hundreds of keV or perhaps a few MeV, is required. Scintillators can be operated in the room temperature conditions and even at higher temperature without much degradation in the spectral performance [5].

The latest technology scintillation detector, Cerium doped Lanthanum Bromide (LaBr₃(Ce)) [18], [19] has shown to provide reasonably good energy resolution comparable to that of semiconductor detectors by operating in room temperature conditions as shown in Figure 8.

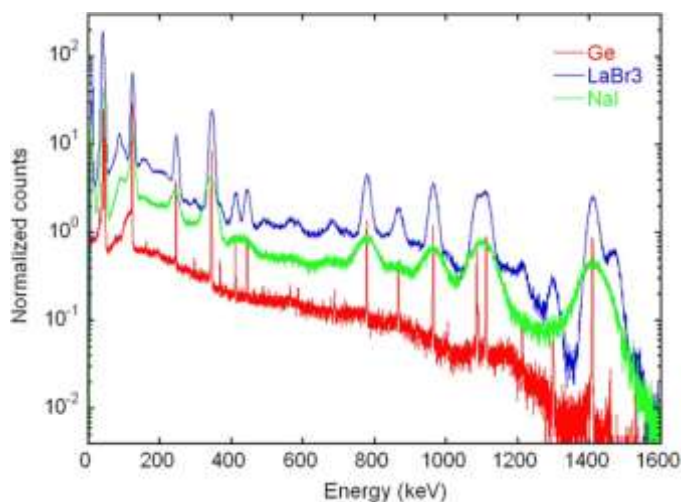


Fig. 8. Spectral performance comparison of Lanthanum bromide with sodium iodide and high purity germanium detector [20].

However, there are drawbacks to lanthanum Bromide detectors, which include internal radioactivity that contributes to spectral counts and a low-energy response that can cause detector resolution to be lower than that of

NaI(Tl) below 100 keV. However, resolving very closely spaced lines could be possible only with semiconductor detectors. Table-1 gives characteristics of scintillation detectors generally used in the scientific measurements.

Table-1. Comparison of various scintillation detectors and its properties

Crystal	Density (g/cm ³)	Light yield (photon/KeV)	Decay time (ns)	Emission Wavelength (nm)	FWHM (%) at 662 KeV
CsI(Tl)	4.51	66	800	550	6.6
NaI (Tl)	3.67	41	230	410	5.6
LaBr ₃ (Ce)	5.3	61	35	358	2.9
BGO	7.1	8.6	300	480	9.0

2.2.1 Scintillator Readout Systems

Scintillation detectors provide output in the form of light, which needs to be converted into electrical form to identify the incident photon energy. The following devices are generally used to convert the visible photons into electrical signal.

1. Photomultiplier tubes (PMT)
2. Photo diodes
3. Silicon photomultipliers (SPM)

2.2.2 Photomultiplier Tubes

Photo multiplier tubes (PMTs) are still the workhorse and generally used to convert the low-level light output into electrical signal by coupling the PMTs with scintillation detectors. PMTs are generally coupled with scintillators using optical compound for better light coupling. The optical light from the scintillators is made to fall on the photocathode of the PMT which converts the light in to electron cloud. These electron clouds are further multiplied by means of acceleration using dynodes which are applied with successively higher potential. The multiplication stages of the PMTs give the gain of the order of $\sim 10^6$. The charge output is read out in the final anode with suitable high voltage coupling capacitor to decouple the high voltage reaching the readout electronics. PMTs are generally bulky and require high voltage ranging from hundreds of volts to few kilo volts (KV) for its electrodes (photocathode and dynodes).

PMTs can be operated either in counting mode or current mode due to larger signal output. The use of photomultiplier still continues and the size and shape [21] of these tubes are made small due to advancement in the PMT technologies. The quantum efficiency of the PMT varies from ~ 10 -50%. PMTs are sensitive to the magnetic field and hence require proper shielding for its operation. Figure 7 gives the schematic representation of the photomultiplier tube.

2.2.3 Photodiodes

A photodiode is a PN junction diode, produces charge carriers when the incident photon with sufficient energy strikes the junction. On the application of the suitable electric field, charge carriers are collected at the electrodes which produces electrical signal. Photodiodes are mainly operated in two different modes namely, photovoltaic mode and photoconductive mode. In photovoltaic mode, zero bias is applied across the diode and the flow of photocurrent is restricted leads to voltage build up. It is used in a system with low noise and where precision is more important than speed. It is similar to solar cells except that the solar cells have large area.

2.2.3.1 Photoconductive mode:

Photoconductive mode of the photodiode is used for light detection. In this mode, the PN junction is reverse biased, which increases the depletion width and reduces the junction capacitance and used in a system where speed is more important than precision. When the light falls on the photodiode, e-h pairs are generated similar to that of ionizing radiation. Photons corresponding to typical scintillation light carries about 3-4 eV of energy, which is sufficient to create e-h pairs in the semiconductor with bandgap energy of 1-2 eV. The quantum efficiency of the conventional photodiodes offers as high as 80% which is several times higher than PMTs and hence provides better energy resolution by operating at very low bias voltages. However, photodiode does not provide charge amplification/multiplication as in PMTs and hence the output signal is orders of magnitude smaller than PMT signal. Photodiodes offer compact size and ruggedness compared to PMTs and the performance does not change with the magnetic field.

2.2.3.2 Avalanche mode:

Avalanche photodiode is a highly sensitive, has similar structure to photodiodes and operated relatively at very high reverse bias voltage. It makes use of internal amplification to achieve the gain due to impact ionization. The charge carriers are accelerated sufficiently between the collations to create the additional charge of e-h pairs along the collection path. This process is similar to one described in proportional counters and thereby provides internal

charge amplification. The internal multiplication helps to distinguish the signal from the noise level and hence improves the energy resolution in pulse mode. This property allows operating avalanche photodiode at lower energies compared to that of photoconductive mode of photodiodes. In this case, the gain multiplication factor is very sensitive to temperature and applied bias high voltage and thereby requiring regulated bias voltage and stable operating temperature. Avalanche photodiodes also provides the quantum efficiency as high as 80%.

2.2.4 Silicon Photomultipliers (SiPM)

The silicon photomultiplier is a multipixel semiconductor photodiode, where the pixels are connected in parallel on common silicon substrate. Each pixel operates in Geiger mode with bias voltage of - 20% more than the breakdown voltage. When a sufficiently high electric field is generated within the depletion region of the silicon, the charge carriers generated in this region will be accelerated to point where it carries sufficient kinetic energy to create secondary charge carriers through impact ionization [22]. In this way, a single photoelectron can trigger self-induced ionization cascade. The silicon will breakdown and become conductive, effectively amplifying the signal. This process is called Geiger discharge [23]. The schematic representation of SiPM is shown in Figure 9.

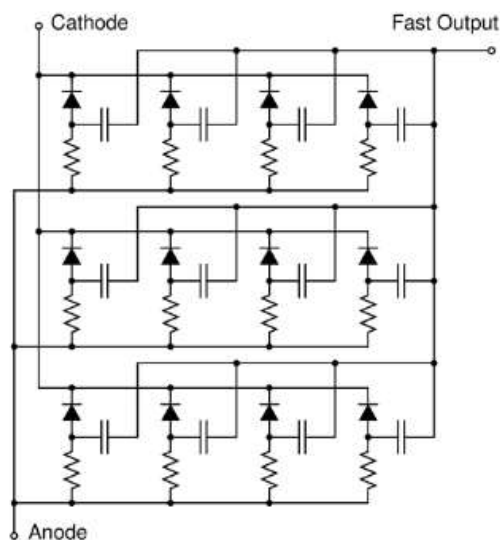


Fig. 9. Schematic representation of SiPM pixel arrays with quenching resistor and summed output (Courtesy SensL).

Each SPM pixel is operated in Geiger mode to achieve high gain. The PN junctions in SPM are designed to withstand the reverse bias beyond its breakdown voltage, creating the necessary high field gradients across the junction. The current flowing through the junction is stopped or quenched using series quenching resistors which limit the current drawn during the breakdown and lowers the reverse voltage below the breakdown voltage. The gain

of each pixel is determined by the charge accumulated in the pixel capacity, which is $\sim 10^6$. The pixel size varies from 15 to 70 μm and the total number of pixels varies from 100-10000 pixels/device [24]. As all the pixels in the SiPM works on a common load and each pixel works as a binary device resulting as a analog detector giving measurement of light intensity.

Therefore, SiPM is capable of detecting low light signal with capabilities of PMT while offering all the benefits of a solid-state device. SiPM is very hot topic of research in recent years and its usage has gained rapidly in the fields of medical imaging, homeland security and high energy physics. These devices are also planned in the future space missions. SiPM is a low cost, robust by the ability to be exposed in room light level without its damage and small physical size. However, there are disadvantages which includes large dark noise (10s of kHz to 1 MHz single photoelectron equivalent), large temperature dependence of breakdown voltage, large cross talk and after pulsing due to charge trapping in silicon substrate. The noise may not be an issue in very high light-level applications or may possibly be mitigated in detector and/or electronics readout design. Thus, there are growing numbers of companies producing these devices and improvements are being carried out in their design to reduce the crosstalk, noise and also in tuning the optical response of these devices. Table-2 gives the comparison of photomultiplier tubes with solid state photo detectors such as photo diode and silicon photomultipliers.

Table-2. Comparison various characteristics of scintillator readout devices such as PMT, Photo diode and SPM

	PMT	Photo Diode		SiPM
		Photo conductive mode	Avalanche mode	
Quantum efficiency	~25 %	~80%	~80%	~20%
Spectral range	Blue/UV	Red	Red	Green
Internal gain	10^6	1	100-1000	10^6
Response time (ns)	Fast	Medium	Slow	Fast
Multiplication noise	Yes	No	Yes	Yes

Sensitive to magnetic field	Yes	No	No	No
Complexity	High (use of HV)	Low	Medium, low noise electronics	Relatively low
Bias requirement	High (1-2 KV)	Low	100-200V	~25V
Temperature sensitivity	Low	Low	High	Low

Each component and combination (scintillator and detector) have its own advantages and disadvantages. One has to use application specific (HEP, Photon Science, Medical Imaging, Industrial Imaging) for his work.

2.3 Semiconductor detectors

The operation of the semiconductor detector is based on the collection of charge carriers induced in the intrinsic region of the detector due to photon interaction by applying suitable bias voltage. The choice of the semiconductor material as a radiation detector depends on the energy range of interest [5], [25]. Semiconductors as detector material came into use in 1960's. Semiconductors were mainly acknowledged for having much higher density than the gas-filled detectors and intrinsic resolution better than the scintillation detectors. Better intrinsic resolution is due to small Fano factor and very efficient conversion of the incident energy into electrical signal. The ionization energy required for silicon is ~ 3.6 eV and for germanium is ~ 2.9 eV, which is one order magnitude smaller than that of gas-filled and scintillators detectors. Variety of semiconductor materials like Si, Ge, HgI₂ [26], CdTe [27], CdZnTe [28] and GaAs [29] were considered for nuclear spectroscopy applications and among these detector materials, silicon and germanium are widely used in practice. The compound semiconductor detectors CdTe, CdZnTe are also increasingly used in spectrometry applications in the high energy X-ray region. However, the other semiconductor detectors, scintillators and proportional counters are still being used for various applications based on the experimental requirement and constraints associated with the application.

Intrinsic semiconductors are pure semiconductor

materials. The intrinsic semiconductor's conduction property is altered by the addition of dopants. The conductivity of a material can be increased by doping it with pentavalent donors, such as phosphorous or arsenic, to create n-type semiconductors. When trivalent impurities like boron are combined with intrinsic semiconductor, p-type semiconductor, often referred to as acceptors, is produced.

2.3.1 Dimond Detectors

Despite being relatively expensive and rare in nature, natural diamond has been used to detect direct and indirect ionising particles from the dawn of the nuclear age, for example, in the early 1940s (1941) [30]. In fact, real diamond was used to make the first solid state radiation detectors since, at the time, finding natural diamond crystals was simpler than making high-quality silicon or other semiconductors [31]. Due to its many exceptional physical and electrical characteristics, diamond is extensively researched and used for the detection of direct and indirect ionizing particles. This material is particularly appealing as a fast-response, high-radiation-hardness, and low-noise radiation detector [32]. In a broad variety of applications, including those needing the capacity to survive hostile environments, diamond detectors are utilized because they are suitable for detecting practically all types of ionizing radiation (such as neutrons, ions, UV, and X-ray) (e.g., high temperature, high radiation fluxes, or strong chemical conditions).

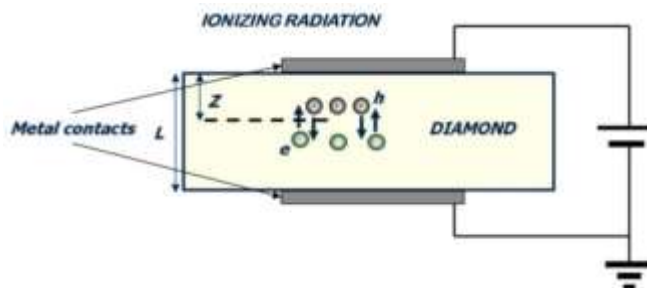


Fig. 10. Schematic view of a typical diamond detector.

A typical diamond detector is a two-terminal device made up of an inherent diamond layer sandwiched between two metal contacts in its most basic form (Figure 10). The diamond detector, also known as a "solid state ionization chamber," is made possible by the high specific resistivity of diamond ($>10^{13}$ cm), which allows for a very simple design of the detector. Between the two electrodes, a biasing voltage (HV) is provided that is typically in the range of 0.5-2 V/m. The detector response may be impacted by excessive HV. The most popular metals for contact deposition are Al, Cr, Ti, Ni, Ag, Au, Pt, and W. Other metals can also be employed. The typical range for metal layer thickness is 30 to 200 nm. A layered metal electrical contact is frequently made up of two (or even three) layers

of various metals, such as Ti/Pt/Au, Cr/Au, etc. In this instance, the thinner metal layer is placed directly on top of the diamond surface, while the thicker metal layer is placed on top of the first metal layer. The latter is used to prevent the first metal layer (such as Cr/Au) from oxidizing or to improve the mechanical and/or thermal properties and also detector bonding/contacting.

The metal-diamond junction can create either Schottky or ohmic connections depending on the metallization process. The former is typically created when a metal layer is simply deposited on top of a diamond surface while still at room temperature (either using sputtering or evaporation process). The result in this situation is a rectifying junction with a typical electrical potential (Schottky barrier). Because of the disparity between the metal and diamond work functions, the size of the barrier (usually 0.5 eV to 1 eV) varies on the metal utilised (Table 3 [33]). Electrons transfer from the substance with the lower work function to the substance with the higher work function when metal and diamond come into contact. The result is a junction at the metal-diamond contact with physical dimensions of a few atomic layers, with one side being slightly positively charged and the other slightly negatively charged.

Table-3. Work function for some of the most used metals for depositing electrical contacts on diamond films.

Element	Work function (eV)
Al	4.1
Ti	4.3
Cr	4.5
Au	5.1
Pt	5.7
Cu	4.65
Ag	4.29
Ni	5.25
W	4.55
Dimond	4.8-5.8

2.3.2 Germanium-based Semiconductor Detectors

Germanium-based semiconductor detectors are most commonly used where a very good energy resolution is required, especially for gamma spectroscopy, as well as x-ray spectroscopy. In gamma spectroscopy, germanium is preferred due to its atomic number being much higher than silicon and which increases the probability of gamma ray interaction. Moreover, germanium has lower average energy necessary to create an electron-hole pair, which is 3.6 eV for silicon and 2.9 eV for germanium. This also provides the latter a better resolution in energy.

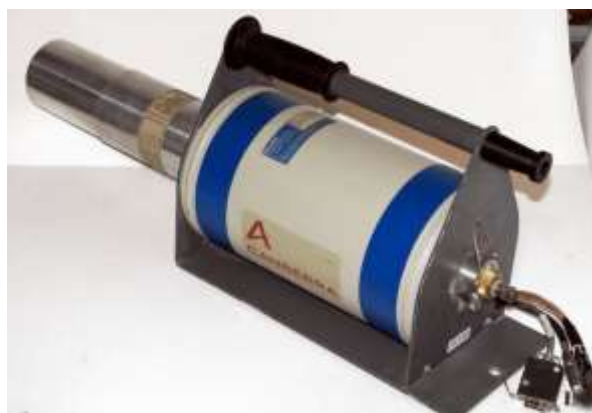


Fig. 11. HPGe detector with LN2 cryostat. [34] (Courtesy: canberra.com)

For use as a radioactivity counter, a large, spotless, and nearly perfect germanium semiconductor is preferable. Large crystals with appropriate purity can be produced, but it is expensive and difficult to do so. Germanium may have a depleted, sensitive thickness of centimeters, but silicon-based detectors can only be a few millimeters thick. As a result, germanium can be employed as a complete absorption detector for gamma radiation up to a few MeV. On the other hand, because thermal excitation noise is so loud at room temperature, the detectors must work at the extremely low temperatures of liquid nitrogen (-196°C) in order to attain optimal efficiency. Since germanium detectors produce the highest resolution currently available, they are used to measure radiation in a variety of applications, including medical applications, radiometric assay, nuclear security, and the safety of nuclear plants as well as personnel and environmental monitoring for radioactive contamination. Figure 11 depicts the HPGe detector made by Canberra.

2.3.2.1 Germanium Detector –Principle of Operation

The following bullet points sum up how semiconductor detectors work [35]:

- Ionizing radiation interacts with the semiconductor material as it enters the detector's sensitive volume (a germanium crystal).
- When a high-energy photon enters the detector, it ionizes the semiconductor atoms and creates electron-hole pairs. The quantity of electron-hole pairs varies in direct proportion to the radiation's energy reaching the semiconductor.
- Since germanium can have a depleted, sensitive thickness of centimeters, they are able to completely absorb high-energy photons. As a result, a number of electrons are moved from the valence band to the conduction band, and an equivalent number of holes are produced in the valence band (up to few MeV).

- A pulse that can be detected in an outside circuit is produced when electrons and holes move to the electrodes under the influence of an electric field.
- This pulse contains data about the energy of the initial incident radiation. The quantity of these pulses in a given amount of time also reveals information about the radiation's intensity.

A photon can be completely absorbed or can always leave some of its energy behind along the way. A 1 MeV photon's total absorption results in 3×10^5 electron-hole pairs [36]. When compared to the total number of free carriers in a 1 cm^3 intrinsic semiconductor, this amount is insignificant. The semiconductor atoms are ionised by a particle as it passes through the detector, creating electron-hole pairs. But at room temperature, thermal excitation predominates in germanium-based detectors. Impurities, irregularities in the structure's lattice, or dopants are the likely culprits. It is highly dependent on the E_{gap} , which is relatively low for germanium ($E_{\text{gap}} = 0.67 \text{ eV}$) and measures the distance between the valence and conduction bands. Some types of semiconductors need active cooling because thermal stimulation causes detector noise (e.g., germanium).

You should be aware that a 1 cm^3 sample of pure germanium at 20°C has roughly 4.2×10^{22} atoms, but it also constantly generates 2.5×10^{13} free electrons and 2.5×10^{13} holes from thermal energy [36]. The signal to noise ratio (S/N) would be quite low, as is evident (compare it with 3×10^5 electron-hole pairs). Arsenic is an impurity that increases electrical conductivity by a factor of 10,000 and gives an additional 10^{17} free electrons in the same volume when added at a concentration of 0.001 percent. The signal to noise ratio (S/N) would be considerably lower in doped material. These detectors must be cooled in order to bring the heat production of charge carriers (and consequently reverse leakage current) down to a manageable level because germanium has a relatively low band gap. Otherwise, leakage current produced noise obliterates the detector's ability to resolve energy [37].

2.3.2.2 Application of Germanium Detectors – Gamma Spectroscopy

Gamma spectroscopy is the study and analysis of gamma ray spectra for scientific and technical purpose, and gamma ray spectrometers are the tools used to observe and gather such data. A sophisticated tool for determining the energy distribution of gamma radiation is a gamma ray spectrometer (GRS). Inorganic scintillators like NaI (Tl) and semiconductor detectors are two detector types that are crucial for the measurement of gamma rays above several hundred keV. The scintillation detector for gamma spectroscopy, which comprises of an appropriate scintillator crystal, a photomultiplier tube, and a circuit for

detecting the height of the pulses produced by the photomultiplier, was discussed in the earlier articles. The efficiency (large size and high density), high precision, and feasible counting rates of a scintillation counter are its advantages. The photo fraction will be high because of the high atomic number of iodine, which causes a significant portion of all contacts to completely absorb gamma-ray energy. Germanium-based semiconductor detectors are most commonly used where a very good energy resolution is required, especially for gamma spectroscopy, as well as x-ray spectroscopy. In gamma spectroscopy, germanium is preferred due to its atomic number being much higher than silicon and which increases the probability of gamma ray interaction. Moreover, germanium has lower average energy necessary to create an electron-hole pair, which is 3.6 eV for silicon and 2.9 eV for germanium. This also provides the latter a better resolution in energy. The FWHM (full width at half maximum) for germanium detectors is a function of energy. For a 1.3 MeV photon, the FWHM is 2.1 keV, which is very low. The comparison of one spectra obtained from NaI(Tl) scintillator and from high purity germanium is shown in Figure 12. In case of Scintillator (NaI(Tl)), the FWHM is $\sim 75 \text{ keV}$ at 1173 keV, but in Germanium the resolution is $\sim 2.35 \text{ keV}$ at 1173 keV. This shows that any gamma ray line which is within 75 keV from 1173 keV line will not be resolved using NaI(Tl).

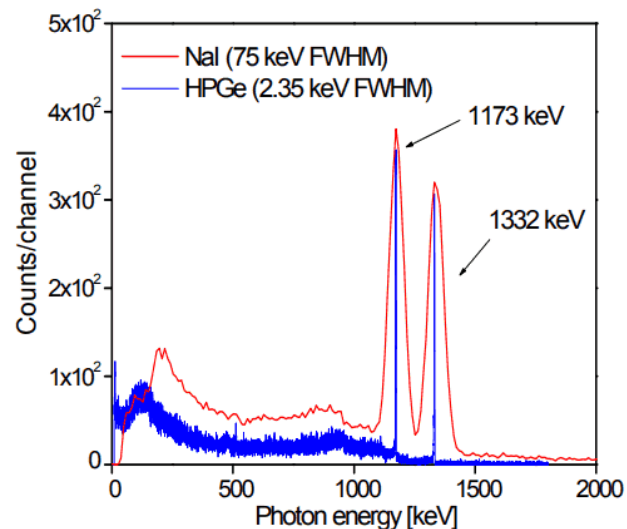


Fig. 12. Comparison of NaI(Tl) and HPGe spectra for cobalt-60. [38]

2.3.3 Cadmium Zinc Telluride detector

A room-temperature semiconductor called cadmium zinc telluride, also known as CZT or CdZnTe, is capable of directly converting x-ray or gamma photons into electrons and holes.

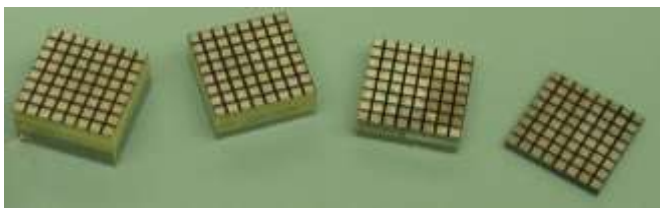


Fig. 13. ORBOTECH make Cadmium Zinc Telluride (CZT) detectors. From left to right, the detectors have volumes of $1 \times 2 \times 2 \text{ cm}^3$, $0.75 \times 2 \times 2 \text{ cm}^3$, $0.5 \times 2 \times 2 \text{ cm}^3$, and $0.2 \times 2 \times 2 \text{ cm}^3$. [39] (picture Courtesy: orbotech.com)

Compared to silicon and germanium detectors, cadmium zinc telluride (CZT) operates at room temperature and has a processing rate of more than 100 million photons per second per mm^2 . This makes it a special semiconductor. Furthermore, CZT's spectroscopic resolution clearly beats that of any scintillator that is currently on the market. CZT is the perfect detector option for medical, industrial, homeland security, and laboratory applications thanks to its special mix of spectroscopy and extremely high-count rate capability at room temperature.

Very thin metalized electrode geometries are placed on the detector surfaces to create CZT detectors (Figure 13). Then, an electrical potential difference between these electrodes and the detector volume is produced. In proportion to the energy of the incoming radiation, many pairs of electrons and holes are produced when ionizing radiation interacts with the CZT crystal.

The positively charged holes and negatively charged electrons subsequently move to the electrodes with the opposite charges, where they are gathered. The preamplifier then picks up the ensuing charge pulse and generates a voltage pulse whose height is related to the incident photon's energy. The pre-amplified signal is then delivered into a shaping amplifier, which amplifies and shapes the signal into a Gaussian pulse. The signal can then be used to create the characteristic spectrum for the incoming photons by feeding it into a common counting system or Multi-Channel Analyzer (MCA). To minimize the size and expense of the readout electronics, we often interface the cadmium zinc telluride CZT-based detector to an ASIC (application specific integrated circuit).

In contrast to silicon and germanium detectors, CZT is a special type of semiconductor. At ambient temperature, cadmium zinc telluride CZT can process more than two million photons per second per mm^2 . Furthermore, CZT's spectroscopic resolution clearly beats that of any scintillator that is currently on the market. Detectors based on scintillators have lower energy resolution. Although cooled semiconductors can provide greater energy resolution, the majority of industrial and medical applications cannot make use of them due to their high installation and maintenance costs, weight, and fragility.

With inexpensive installation and lifetime costs as well as good energy resolution, CZT fills the gap between scintillator-based detectors at one end and high-maintenance germanium detectors at the other.

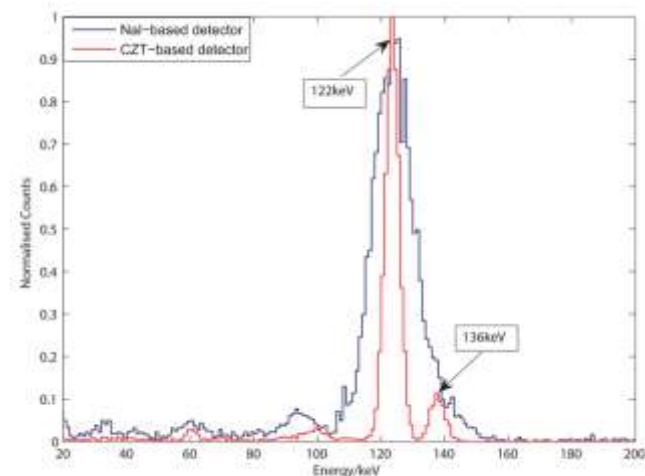


Fig. 14. Comparison of energy spectra of ^{57}Co obtained by CZT-based detector and NaI-based detector. [40]

Figure 14 compares the energy spectra for the ^{57}Co radioactive source, in from the CZT-based and NaI-based detectors. While NaI crystal cannot, the CZT detector can clearly differentiate the 122 keV photopeak from the 136 keV of ^{57}Co . To facilitate comparison, the counts have been normalized.

2.3.4 Silicon Detectors

The real use of silicon as photo detector was made possible by the introduction of planar technology which led to the fabrication of silicon detectors by Kemmer in 1980 [41] and Pantazis 1984 [42]. Planar technology consists of series of processing steps on a crystalline silicon wafer and very recently, implants near the top and bottom sides. The planar diode fabrication follows formation of SiO_2 layer on the Si bulk, selective removal of SiO_2 , introduction of dopant atoms into wafer surface and dopant diffusion into silicon. Combination of these steps can produce any type of complex device on the silicon bulk. The schematic of making planar technology detector is shown in Figure 15. Silicon planar technology is commonly used in the fabrication of microelectronic circuits [43, 44]. Subsequently, there is lot of development in the last few decades in the silicon detector technologies yielding new detector configurations such as Si PIN, Si Strip and pixilated detectors, charge coupled device (CCD) and Silicon Drift Detector (SDD). These silicon detector configurations are used in vast number of applications and fields. Each of these technologies is briefly described in the following subsections.

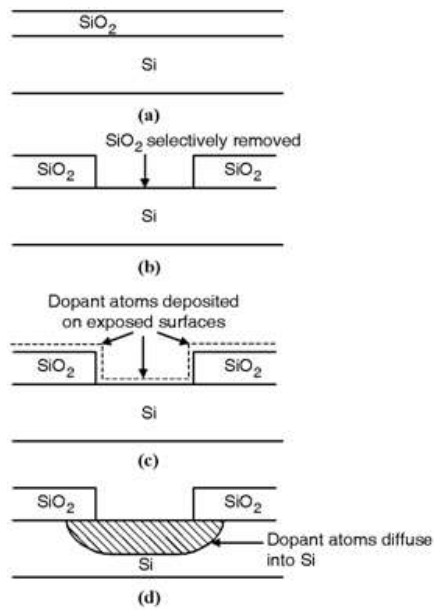


Fig. 15. Schematic representation of making of silicon planar technology, (a) Oxidation of silicon, (b) Selective removal of oxide layer, (c) Introduction of dopant atoms and (d) Diffusion of dopant atoms into silicon [45].

2.3.4.1 Si PIN Diode Detector

Silicon detectors were used in the form of Si PIN diode for the radiation detection in 1980's and 1990's as discussed in Kemmer (1980) [41] and Pantazis (1994) [42]. Si PIN diode detectors have been consistently used in various applications including in the space/planetary missions for detecting X-rays in the energy range of 1 - 25 keV until the Silicon Drift Detector technology was available for the researchers. These detectors are available in different sizes starting from 5 mm² to 25 mm² and thickness ranging from few microns to few hundred microns. Generally, the Si PIN diodes with thickness \leq 500 micron are used for detecting X-rays in the energy range of 1 - 25 keV with reasonably good energy resolution. X-ray spectrometer with 6 mm² area, 500 micron thick [33] provides the energy resolution of \sim 220 eV at 5.9 keV (^{55}Fe X-ray source) when the detector is cooled to -40°C for the pulse peaking time of 2.4 μs . In case of larger area Si PIN detectors (25 mm²), the energy resolution is $>$ 300 eV [46] for the same detector thickness due to larger capacitance of a larger area detector.

Si PIN detectors provide good energy resolution relatively at low count rates ($<$ 10^4 counts/s) due to larger detector capacitance and are not generally suitable for high count rate applications. These detectors are available in the form of standalone modules consisting of Si PIN chip, JFET which is part of first stage of charge readout amplifier to improve signal/noise ratio, and the Peltier cooler to cool the detector to lower operating temperatures. Front side of these detector modules are covered with 8/13/25 micron

thick beryllium (Be) window to avoid any stray light falling on to the detector and also helps to maintain conditioned environment inside the module when the detector is cooled to lower temperatures. The 8-micron thick Be window reduces the detector efficiency to 30% for 1 keV X-ray photon. The schematic representation of one such module is shown in Figure 16 and its spectral performance is shown in Figure 17.

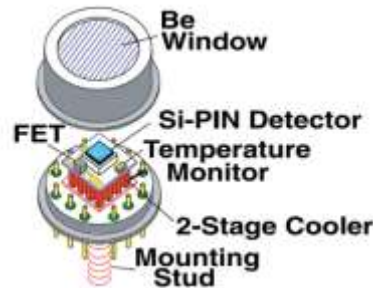


Fig. 16. Schematic representation of constituents of SiPIN detector module [46] (Courtesy AMPTEK)

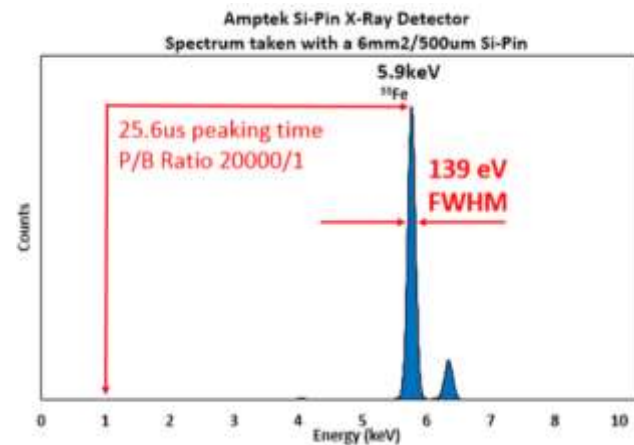


Fig.17. A sample ^{55}Fe spectrum acquired using 500-micron thick SiPIN detector module. [46] (Courtesy AMPTEK)

2.3.4.2 Si (Li) detectors

The brains of solid-state X-ray spectroscopy devices are silicon lithium X-ray detectors. These detectors were created using some of the most meticulously planned manufacturing techniques ever [47]. They are p-i-n devices made by drifting of p-type silicon or compensating for lithium. These detectors are made in accordance with stringent quality requirements, which is necessary to guarantee a high level of performance and outstanding long-term dependability. A low noise Integrated Transistor Reset Preamplifier and a liquid nitrogen cryostat are other essential components of the Si (Li) x-ray detector system (I-TRP). These detectors, along with low energy germanium detectors and Silicon Drifted Detectors (SDDs),

have a niche in the market for x-ray applications. As shown in Figure 18, Si(Li) detectors, which can be produced with thicknesses up to 5 mm, have a substantially higher stopping power than SDDs (max. 500 μ m) and can be employed up to higher energy x-rays.

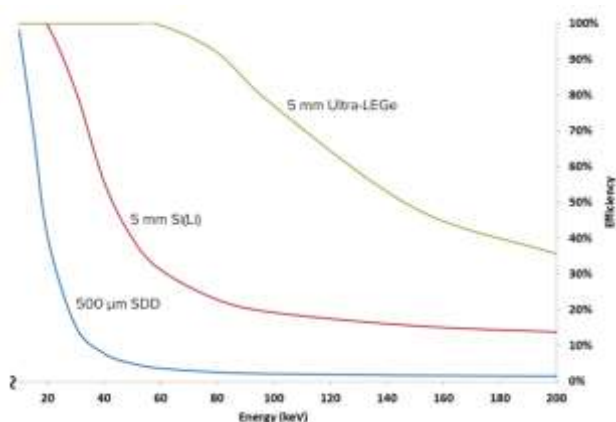


Fig. 18. Comparison of high-energy efficiency Germanium vs. Silicon [48] (Courtesy MIRION technologies)

But for a given detector thickness, silicon has a lower stopping power than germanium. However, compared to germanium, silicon has distinctive x-rays at significantly lower energy (about 1.7 keV) (10-11 keV). The generated x-rays are consequently less likely to escape the detector volume, which lessens the prominence of the escape peak. This indicates that for a Si (Li) detector in comparison to an HPGe detector, the ratio of the full energy peak to the escape peak is 2-3 orders of magnitude larger. Additionally, the germanium x-rays are located in the range of interest for various investigations or applications, which is between 10 and 11 keV. The spectra and the analysis are made more difficult by the absorption edges of germanium in the region of interest. Si (Li) detectors are utilized in a wide range of applications, such as x-ray fluorescence, x-ray microanalysis, PIXE, x-ray diffraction, etc., and cover an energy range from a few hundred eV to above 50keV.

2.3.4.3 Silicon Strip Detectors (SSD)

Silicon Strip Detector is a type of position sensitive silicon detector obtained by segmenting larger detector into small sub detectors and each sub detectors are connected with individual readout electronics. The charge induced due to photon interaction will be detected in the multiple chains of readout electronics and thereby the position information can be obtained.

In early 1980's, G Lutz and J. Kemmer pioneered the development of silicon strip detectors. The radiation hardened silicon strip detectors were available from 1990's and subsequently, the technology transfer to industry took place for bulk production. The silicon strip detector can be created by patterning larger p-n junction of a PIN diode into an array of long and narrow strip like structure forming

individual p-n junctions as shown in Figure 19. The strips usually extend the full length of the sensor. The biasing of the strips is fed from a shared common power supply. When the reverse bias is applied to all the junctions together, individual depletion layers overlap and device behaves like large PIN diode with multiple readout electrodes. The width of the strip is in the order of few tens of microns and the pitch between the strips varies from - 50 μ m up to several hundreds of microns [49, 50]. Strips in one side and planar contact on other side forms single sided strip detector (SSSD), which can provide 1 D - position sensing capability.

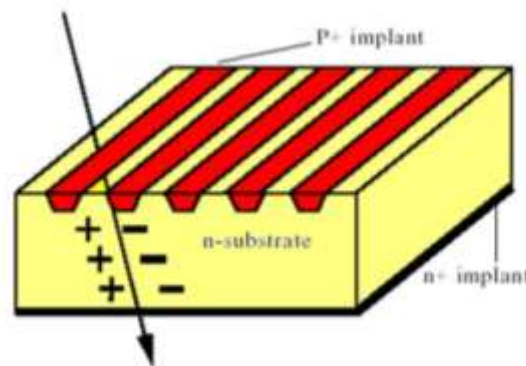


Fig. 19. Single side silicon strip detector.

If the strip patterns are established on both the sides of the silicon sensor with crossed strips known as double sided silicon strip detector (DSSD). With the crossed pattern, by reading the signal charge due to both electrons and holes in the opposite electrodes, one can estimate the position accurately with 2D-position capability. The layout representation of 2D strip detector is shown in Figure 20.

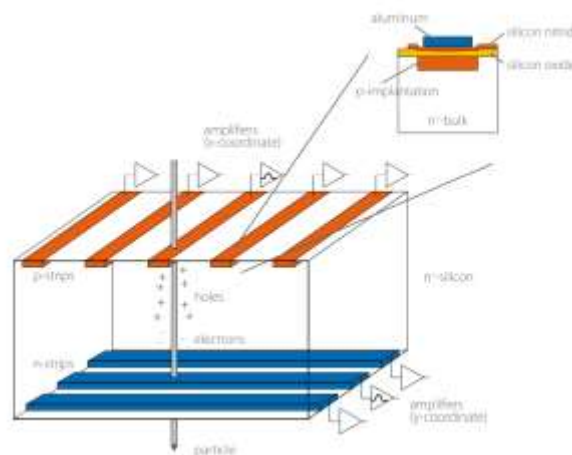


Fig. 20. Layout of double sided (2D) silicon strip detector [51].

SSD's are also widely used for tracking charged particles

and there are SSD based systems available providing 20 position resolution as low as $1 \mu\text{m}$. Currently, these detectors are available in wafer size of about 4-5 inches and combining many of such detectors will provide large area, essential for many scientific applications. Making such large size is possible due to simple electrode structures. Large number of these detectors are being used in ATLAS experiment at CERN [52] with silicon active area are $>150 \text{ m}^2$ and in CMS experiment of LHC [53] with active area of 200 m^2 . Silicon strip detectors are also employed as gamma detector in space-based Compton telescopes, GLAST with active area of $\sim 80 \text{ m}^2$ [54]. Strip detectors are seldom used for spectroscopic applications due to larger capacitance of the charge collecting electrodes which results in poor energy resolution.

2.3.4.4 Pixel Detectors

In case of silicon strip detector, the detector will not be able to assign the position unambiguously if there are multiple events within the readout period. This drawback is due to the longer electrode structure. In such cases, pixel detectors have to be used. Instead of longer strips, segment the strips in both the sides, becomes pixel detectors. This configuration increases 2D resolution and also provides better energy resolution due smaller electrode capacitance. Such pixilated detector calls for large number of readout chains and hence the conventional discrete electronics-based readout will be impractical. Hence, it is essential to have Application Specific Integrated Circuit (ASIC) based readout system for the pixilated detectors.

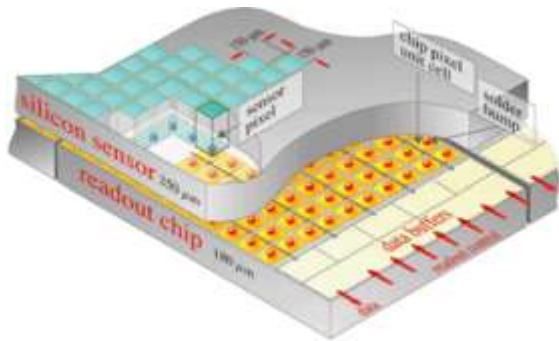


Fig. 21. Pixel silicon detector used in the CMS experiment (3D-model) [55].

2.3.4.5 Fully Depleted p-n CCD

The concept of charge coupled device (CCD) was originally introduced as a imaging device in video cameras. The principle of operation is based on the storage and transport of charge. Subsequently, the modified version of the CCD was proposed for detecting radiation in the form of fully depleted CCDs [56, 57] with on-chip FET [58]. The basic schematic representation of fully depleted p-n CCD is shown in Figure 22.

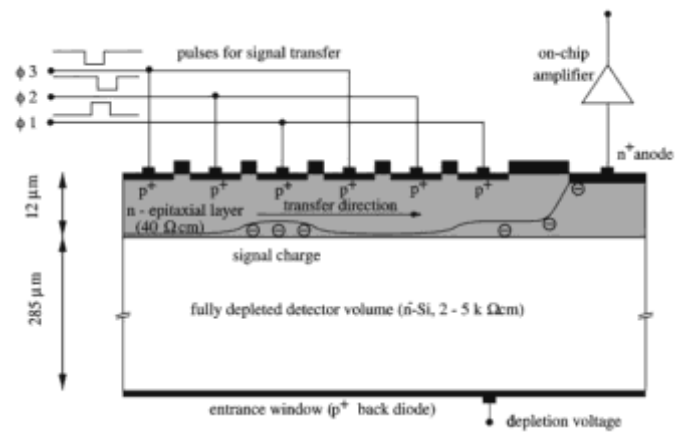


Fig. 22. Schematic representation of p-n CCD cut through view (courtesy PN Sensor) [59]

Fully depleted p-n CCDs are based on the sideward depletion of high resistivity silicon theory, which was put forth in 1983 and 1984 for silicon drift detectors. The fundamental idea was altered and tailored to create p-n CCDs in the ensuing years [59].

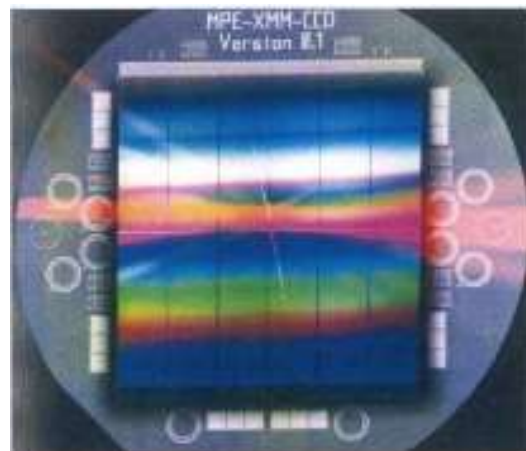


Fig. 23. The photographic view of p-n CCD built with sensitive area of $6 \times 6 \text{ cm}^2$, flown in XMM-Newton satellite missions [59].

It is built on a high ohmic n-type silicon bulk as that of other silicon detector with a n-type epitaxial layer and a matrix of p+n strips and perpendicular p+ implants on the upper surface. When X-ray photon strikes, the electrons are drifted towards potential minimum wells under the p+ contacts called transfer registers. The holes are absorbed by the back contact. The electrons in the potential well are then transferred to the readout electrode by changing the biasing conditions of the transfer registers. In this configuration, the charge readout speed is increased as the single-phase sequencing is sufficient to transfer the charge to the neighboring register and this is achieved by means of structuring the potential minima for electrons at three different depths in the n-type epitaxial layer. The major advantage of this configuration is that the detector

efficiency improves greatly by operating in fully depleted mode compared to MOS CCDs of same thickness.

The fully depleted region of the silicon bulk makes it attractive to use in the X-ray spectroscopy. P-n CCDs are generally used for X-ray imaging as it has the limitation of using in photon counting mode at high count rates due to sequential readout. In X-ray imaging, the position resolution is very important and this is mainly determined by the strip spacing which is of the order few tens of microns. The charge spread during the charge integration and transfer is made negligible in the fully depleted p-n CCDs.

Though the functional p-n CCDs were available in 1993, the first large area and large depletion p-n CCD was made at Max Planck Institute for extraterrestrial physics together with semiconductor laboratory involving PN Sensor. The fabricated sensitive area was $6 \times 6 \text{ cm}^2$ with pixel size of $150 \mu\text{m} \times 150 \mu\text{m}$ having depletion thickness of $300 \mu\text{m}$. This device provided unprecedented quantum efficiency in the energy range of 100 eV to 15 keV. This sensor was successfully flown in XMM-Newton satellite missions [60, 61] and the photographic view of the same is shown in Figure 23.

In recent years, p-n CCD are available in multiple pixel sizes from $36 \mu\text{m} \times 36 \mu\text{m}$ up to $150 \mu\text{m} \times 150 \mu\text{m}$, depletion depth up to $450 \mu\text{m}$ and the active area reaching from 1 cm^2 to 3 cm^2 .

2.3.4.6 Silicon Drift Detector (SDD)

Silicon Drift Detector (SDD) is a new technology silicon photo detector with unique electrode structure and offers low detector capacitance compared to planar Si PIN detector of same area. This yields low noise even at shorter shaping times and hence, SDDs can be used at much higher count rates with desired energy resolution. The concept of SDD was introduced in 1984 by Gatti and Rehak who presented the concept and the experimental results [62]. The concept was based on the sideward depletion. SDD was initially proposed for position measurement and considered as a replacement for gas chambers in the form of solid-state device. In his work, it was observed that detector capacitance is independent of detector area. In 1985, Rehak and Gatti [63] have shown the use of SDDs for energy measurements rather than position measurement with SDD in circular form. In these SDDs, the drift electrodes are made on both the sides to form the radial electric field. The planar electrode concept in SDD was introduced in 1987 by Kemmer [64] with planar contact on one side and drift electrodes on the opposite side. As discussed in the earlier chapter, the fabrications of planar contacts are easier to manufacture. This technique also provides very thin dead layer in the entrance window where only X-ray photons are allowed to enter in to the detector, which is important for X-ray spectroscopy. The first good

quality SDD for laboratory application was produced in 1995 for EDS and XRF measurements [65]. In the last two decades, SDDs are being optimized to achieve very good spectral energy resolution in various types and sizes [66, 67, 68, 69]. Significant research work has been carried out in the SDD readout techniques [70, 71, 72] aiming at improving the energy resolution by reducing the contribution of electronics noise. In recent times, it is shown that SDDs with advanced readout electronics can provide energy resolution close to Fano limit.

2.3.4.7 Working principle of SDD

In the conventional PIN photo detector, the ohmic n+ contact extends to the full area of the silicon bulk on one side and the potential distribution is shown in Figure 24 (a). In Figure 24 (b), n+ contact introduced with p+ electrodes on both the sides to achieve the depletion of the bulk and when the bias at n+ contact is increased, creating a potential minimum at the center of the bulk with small un-depleted zone near the n+ region as shown in Figure 24 (c).

The working principle of drift detector is understood from the sideward depletion concept. In case of SDD, an additional electric potential is applied on both sides to force the electrons to drift towards the n+ electrode for the signal readout as shown in Figure 25.

The P⁺ electrodes are implanted on both sides to achieve this. These electrodes are appropriately biased to produce the electric field line in Figure 26.

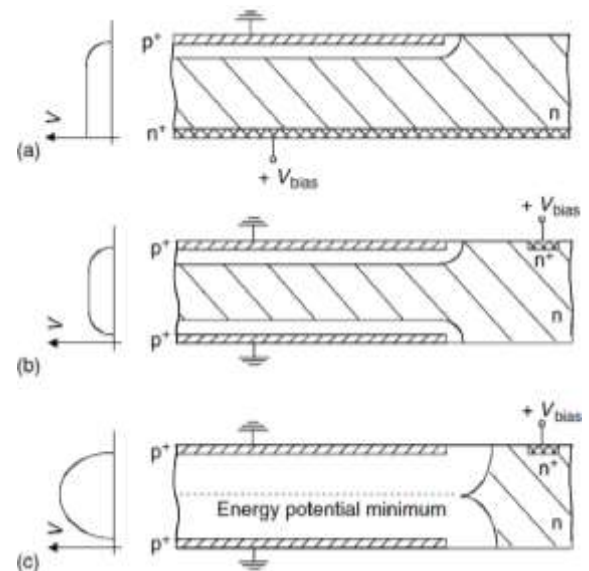


Fig. 24. Schematic representation of sideward depletion concept [62].

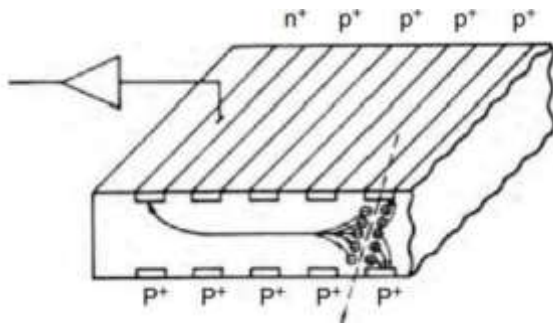


Fig. 25. Schematic representation of working principle of silicon microstrip detector [62].

When a photon interacts with the detector's active volume, the electrons are directed towards the anode, and the holes are attracted to the closest p+ electrodes by the negative bias that is provided to those electrodes. The region close to the collecting anode, the bottom of the potential channel is shifted towards the surface where the anode is present by suitably biasing the opposite electrodes. The electron cloud gives an electric pulse in the anode and the drift time of the electron cloud along with the signal due to holes can be used to derive the measure of the position of the photon interaction [65].

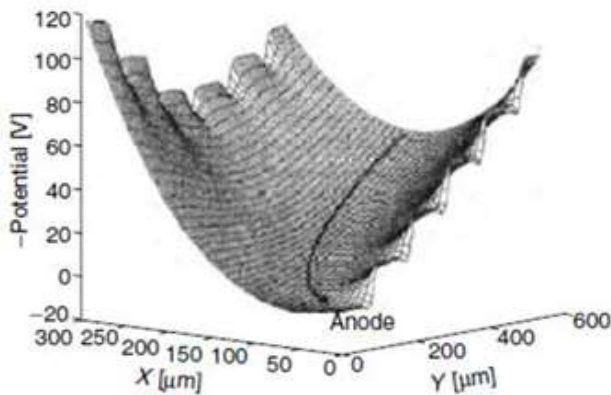


Fig. 26. The electron guiding potential distribution in the drift region of the SDD pointing towards the anode [62].

The signal due to electron charge will give the energy of the photon. The important finding of this sideward depletion concept is that the detector capacitance is the anode capacitance whose value is independent of the detector area. The anode capacitance is of the order of few hundred fempto farad. The low detector capacitance provides low noise at lower shaping times and thereby the system can be used for high count rate applications.

2.3.4.8 SDD for X-ray measurements

SDDs are ideally suited for X-ray spectrometry due to its low detector capacitance along with the low noise readout system enables to achieve the energy resolution close to the Pano limit. In the sideward depletion SDD

concept, the areas between the p+ strips on the surface are covered with SiO₂ layer. There is fixed positive charges in the SiO₂ layer causing the potential distribution downward from the detector surface creating potential minima. These sites could collect the signal electrons generated during the photon interaction, in the low energy range < 5 keV [73].

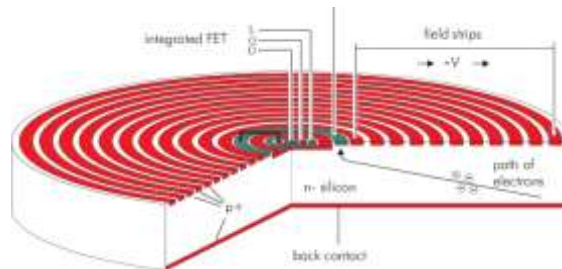


Fig. 27. Schematic representation of a circular SDD with anode at the center (courtesy KETEK, GmbH) [75].

To overcome this limitation at lower X-ray energies, a suitable design topology has been implemented with a thin continuous entrance window without oxide layer gaps [74]. Also, the point anode is kept in the center forming a circular detector that minimizes any signal loss due to the travel length of the signal electrons. The circular SDD optimized for energy measurement is shown in Figure 27. Circular SDDs have concentric rings around the point anode, which are applied with progressively higher reverse bias voltages, which guide the photoelectrons into a "point" anode. The drift field with respect to the point anode at the center is shown in Figure 28.

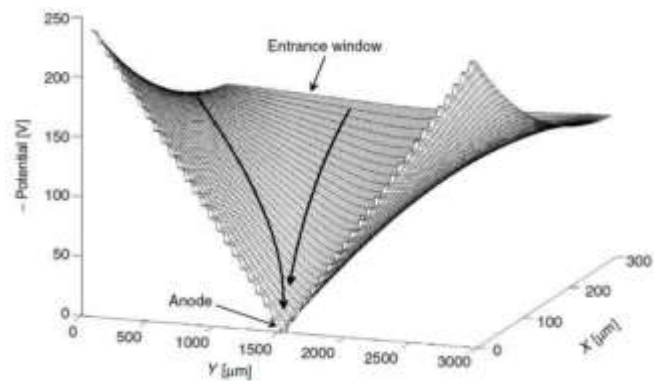


Fig. 28. The possible electron path (field line) inside the SDD with 300-micron thickness [75].

The bias voltage required for the successive p+ electrodes are derived from a single high voltage applied at the outer electrode by using resistive divider which is part of the SDD chip. The inner ring close to the anode and the back contacts are applied with separate bias voltages. The capacitance of the point anode is ~200 ff. The p+ back contact acts as entrance window for the radiation to be

detected is made of a shallow p+ implantation with thickness of the order of few tens of nano meters [76] which allows to achieve the low energy threshold of few hundred eV. The quantum efficiency of such SDD with few tens of nm of dead layer for 450 and 900-micron thick detector is reported in [77]. It is shown that the quantum efficiency of > 40% could be achieved for incident energies more than 200 eV as shown in Figure 29.

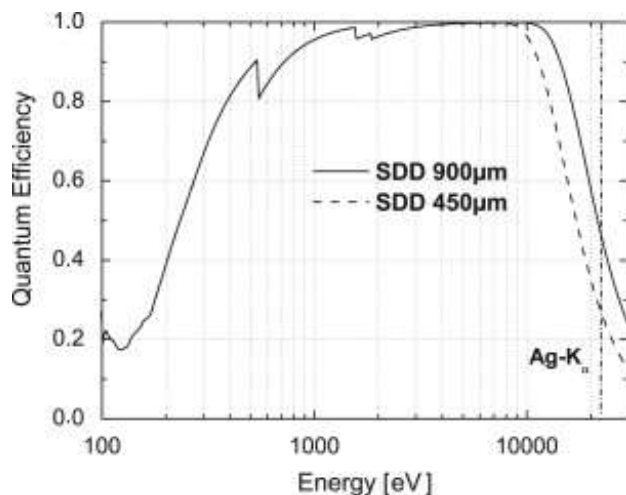


Fig.29. Quantum efficiency of a 450 and 900-micron thick SDDs with thin dead layer [77].

3 Conclusions

In this review paper, the working principle and various types of radiation detectors are discussed. This paper also describes technologies adapted over past several decades in X-ray studies, their working principle, charge formation and readout techniques. The suitability of these detectors for the desired energy range is described by comparing their performances and also giving their merits and demerits. The use of silicon detectors in various applications is also described.

Acknowledgment

We acknowledge the financial support by the Indian Space Research Organization, Department of Space, Government of India. We also thank prof. Santosh Vadawale, Dr. M.Shanmugam, Mr. N.P.S Mithun for discussions on the radiation detectors working principle. This work is a part of the Ph.D. work of Arpit Patel. Director PRL, Head of Planetary Science Division, PRL, and Dean DDU, Nadiad are gratefully acknowledged for constant encouragement during the work.

References

[1] M. Uthman, F. Shaibu, N. Bara'u Gafai and I. Labaran, "5G Radiation and COVID-19: The Non-Existent Connection," International journal of

research in electronics and computer engineering, pp. 34-38, June- 2020.

- [2] <https://www.ans.org/nuclear/radiation/>
- [3] <http://nuclearsafety.gc.ca/eng/resources/radiation/introduction-to-radiation/types-and-sources-of-radiation.cfm>.
- [4] J. M. F. dos Santos and et al, "The development of portable gas proportional scintillation counters for X-ray spectrometry," X-ray spectrometry, vol. 30, pp. 373-381, 2001.
- [5] G. F. Knoll, Radiation Detection and Measurement, John Wiley & Sons, 3rd edition, 1999.
- [6] http://www-physics.lbl.gov/~spieler/Heidelberg_Notes, 2001..
- [7] www.XCounter.com.
- [8] S. Mukhopadhyay and Mason, "Smart Sensors," Measurement and Instrumentation; School of Engineering and Advanced Technology, Massey: Palmerston North, New Zealand., 2013.
- [9] V. Kandan, M. Hassan, N. Omar, H. Shahar, F. Mohamad, M. Karim, S. Sani, D. Bradley and N. Noor, "Advanced glow curve analysis of fabricated fibres for various sources of ionizing radiation.," Radiat. Phys. Chem. , vol. 178, no. 108981, 2021.
- [10] M. Jamil, "Effect of gamma irradiation on magnetic gadolinium oxide nanoparticles coated with chitosan (GdNPs-Cs) as contrast agent in magnetic resonance imaging.," Radiat. Phys. Chem., vol. 165, no. 108407, 2019.
- [11] F. J. Mettler and M. Guiberteau, "Essentials of Nuclear Medicine Imaging: Expert Consult," Online and Print; Elsevier Health Sciences: Philadelphia, PA, USA, , 2012.
- [12] A. Kaur, S. Sharma and B. Mittal, "Comparison of sensitivity of Geiger Muller counter and ionization chamber based survey meters.," Journal of Nuclear Medical, vol. 53, no. 2607, 2012.
- [13] J. M. F. a. e. dos Santos, "The development of portable gas proportional scintillation counters for X-ray spectrometry," X-ray spectrometry, vol. 30, pp. 373-381, 2001.
- [14] <https://physicsopenlab.org/2017/07/23/x-ray-proportional-counter-2/>.
- [15] A. Braby and G. Badhwar, "Proportional counter as neutron detector," Radiation measurements, vol. 33, pp. 265-267, 2001.
- [16] P. Habrman, "Directional Geiger-Müller detector with improved response to gamma radiation.," Journal of instrumentation, vol. 14, p. P09018, 2019.
- [17] https://www.hamamatsu.com/resources/pdf/etd/PMT_handbook_v3_aE-Chapter7.pdf.
- [18] P. Dorenbos, J. T. M. de Haas and C. W. E. van Eijk, "Gamma-Ray Spectroscopy with a 19 x 19 mm³ LaBr₃:0.5%Ce³⁺ Scintillator," IEEE Transactions on Nuclear Science, vol. 51, no. 3, pp. 1289-1296, 2004.
- [19] S. Mukhopadhyay, "High-Resolution Room Temperature Spectroscopy with," Nuclear Science and Engineering, vol. 151, 2005.

- [20] E. Seabury, J. C. Wharton and A. J. Caffrey, "Response of a LaBr₃(Ce) Detector to 2-11 MeV Gamma Rays," IEEE Nuclear Science Symposium, 2006.
- [21] <http://www.hamamatsu.com/jp/en/3001.html>.
- [22] <http://www.sensl.com/downloads/ds/TNIntroSPMTech.pdf>.
- [23] <http://www.ketek.net/products/sipm-technology/working-principle/>.
- [24] <http://www.ketek.net/products/siprn/pm6660/>.
- [25] G. Lutz, "Semiconductor Radiation Detectors," in Springer, 1999.
- [26] Y. J. Wang, J. S. Iwaczyk and W. R. Graham, "Evaluation of Hgh detectors for lead detection in paint," IEEE Trans. on Nucl. Sci., vol. 40, no. 4, pp. 846-850, 1993.
- [27] M. R. Squillante and G. Entine, "New applications of CdTe nuclear detectors," Nucl. Instr. and Meth. A, vol. 322, no. 3, pp. 569-574, 1992.
- [28] M. McConnell and et al, "Three-dimensional imaging and detection efficiency performance of orthogonal coplanar CZT strip detectors," Proceedings of SPIE, vol. 4141, pp. 157-167, 2000.
- [29] G. Bertuccio and et al, "Pixel X-ray detectors in epitaxial gallium arsenide with high-energy resolution capabilities," IEEE Trans. on Nucl. Sci., vol. 44, no. 1, pp. 1-5, 1997.
- [30] R. Hostader, "Crystal counters," Nucleonics, vol. 4, no. 29, 1949.
- [31] A. Paoletti, A. Tucciarone and et al, "The physics of diamond," In Proceedings of the International School of Physics Enrico Fermi—Course, Varenna, Italy,, 1996.
- [32] C. E. Nebel, "Electronic properties of diamond," Semiconductor Science Technology, vol. 18, pp. S1-S11, 2003.
- [33] J. Rivière, "Solid State Surface Science," Marcel Dekker: New York, NY, USA, , vol. 1, no. ISBN 0824760174 9780824760175. , 1969.
- [34] www.canberra.com.
- [35] <https://www.radiation-dosimetry.org/what-is-principle-of-operation-of-hpge-detectors-definition>.
- [36] J. R. Lamarsh and A. J. Baratta, Introduction to Nuclear Engineering, 3d ed., Prentice-Hall, 2001.
- [37] W. M. Stacey, Nuclear Reactor Physics, John Wiley & Sons, 2001.
- [38] B. Hyun, Radioisotopes and Radiation Methodology I, II., Lecture Notes., McMaster University, Canada..
- [39] www.orbotech.com.
- [40] F. Weng, S. Bagchi, Q. Huang and Y. Seo, "Design Studies of a CZT-based Detector Combined with a Pixel-Geometry-Matching Collimator for SPECT Imaging," IEEE Nuclear Science Symposium conference record. Nuclear Science Symposium., no. NSSMIC.2013.6829458., pp. 1-4, 2014.
- [41] J. Kemmer, "Fabrication of low noise silicon radiation detectors by the planar process," Nucl. Instr. and Meth. A, vol. 169, pp. 499-502, 1980.
- [42] J. A. Pantazis and et al, "New, High Performance Nuclear Spectroscopy System Using Si- PIN Diodes and CdTe Detectors," IEEE Trans. on Nuc. Sci., vol. 41, no. 4, pp. 1004-1008, 1994.
- [43] W. R. Runyan and K. Bean, Semiconductor Integrated Circuit Processing Technology, MA: Addison-Wesley, 1990.
- [44] S. Sze, VLSI Technology, 2nd ed., New York: McGraw-Hill Book Company, 1988.
- [45] <https://www.electronics-tutorial.net/CMOS-Processing-Technology/planar-process-technology/>.
- [46] http://www.amptek.com/products/xr-1_OOcr-si-pin-x-ray-detector/.
- [47] <https://www.mirion.com/products/sili-detector-x-ray-silicon-lithium-detector-for-x-ray-spectroscopy>.
- [48] https://mirion.s3.amazonaws.com/cms4_mirion/files/pdf/spec-sheets/c40120_sili_det_for_x-ray_spect_ss_2.pdf.
- [49] J. Kemmer and G. Lutz, "New Structures for Position Sensitive Semiconductor Detectors," Nucl. Instr. Meth. A, vol. 273, no. 2-3, pp. 488-598, 1988.
- [50] A. Peisert, "Silicon Microstrip Detectors," DELPHI 92-143 MVX 2, CERN, 1992.
- [51] CMS Tracker Collaboration, "Supply of Silicon Micro-Strip Sensors for The CMS Silicon Strip Tracker," IT-2777/EP/CMS, 2000.
- [52] R. Richter and et al, "Strip detector design for ATLAS and HERA-B using two-dimensional device simulation," Nucl. Instr. Meth. A, vol. 377, no. 2-3, pp. 412-421, 1996.
- [53] CMS Tracker Collaboration, "Supply of Silicon Micro-Strip Sensors for The CMS Silicon Strip Tracker," IT-2777/EP/CMS, 2000.
- [54] F. Hartmut and W. Sadrozinski, "GLAST, a Gamma-Ray Large Area Space Telescope," Nucl. Instr. Meth. A, vol. 466, no. 2, pp. 292-299, 2001.
- [55] F. Hartmann, "Evolution of Silicon Sensor Technology in Particle Physics," Springer Tracts in Modern Physics, vol. 231, 2009.
- [56] L. Stroder et al, "Device Modelling of fully depletable CCDs," Nucl. Instr. Meth. A, vol. 253, no. 3, pp. 386-392, 1987.
- [57] L. Stroder et al, "The MPI/AIT X-ray imager (MAXI) - High speed pn-CCDs for X-ray detection," Nucl. Instr. Meth. A, vol. 288, no. 1, pp. 227-235, 1990.
- [58] E. Pinotti et al, "The pn-CCD on-Chip Electronics," Nucl. Instr. Meth. A, vol. 326, no. 1-2, pp. 85-92, 1993.
- [59] <http://www.pnsensor.de/Welcome/Detectors/pn-CCD/index.php>.
- [60] L. Struder et al, "X-ray pn-CCDs on the XMM Newton Observatory," Proc. SPIE, vol. 4012, pp. 342-352, 2000.

- [61] L. Stroder et al, "The European photon imaging camera on XMM-Newton: The pn-CCD Camera," *Astronomy and Astrophysics*, vol. 365, pp. L18-L26, 2001.
- [62] E. Gatti and P. Rehak, "Semiconductor drift chamber- An application of a novel charge transport scheme," *Nucl. Instr. and Meth. A*, vol. 225, no. 3, pp. 609-614, 1984.
- [63] P. Rehak et al, "Semiconductor drift chambers for position and energy measurements," *Nucl. Instr. Methods A*, vol. 235, no. 2, pp. 224-234, 1985.
- [64] J. Kemmer et al, "Low capacity drift diode," *Nucl. Instr. and Meth. A*, vol. 253, no. 3, pp. 378-381, 1987.
- [65] T. Pantazis et al, "The historical development of the thermoelectrically cooled X-ray detector and its impact on the portable and hand-held XRF industries," *X-ray Spectrometry*, vol. 39, no. 2, pp. 90-97, 2009.
- [66] J. Kemmer and G. Lutz, "New semiconductor detector concepts," *Nucl. Instr. Meth. A*, vol. 253, no. 3, pp. 365-377, 1987.
- [67] <http://www.pnsensor.de/Welcome/Detectors/SDD/>.
- [68] G. Carini et al, "Performance of a thin-window silicon drift detector X-ray fluorescence spectrometer," *IEEE. Trans. Nucl. Sci.*, vol. 56, no. 5, pp. 2843-2849, 2009.
- [69] G. Zampa, A. Rashevsky and A. Vacchi, "The X-ray spectroscopic performance of a very large area silicon drift detector," *IEEE. Trans. Nucl. Sci.*, vol. 56, no. 3, pp. 832-835, 2009.
- [70] G. Bertuccio, M. Sampietro and A. Fazzi, "High resolution X-ray spectroscopy with silicon drift detectors and integrated electronics," *Nucl. Instrum. Meth. A*, vol. 322, no. 3, pp. 538-542, 1992.
- [71] P. Lechner, A. Pahlke and H. Soltau, "Novel high-resolution silicon drift detectors," *X-Ray Spectrometry*, vol. 33, no. 4, pp. 256-261, 2004.
- [72] <http://www.Pnsensor.de/Welcome/Detectors/SDD/index.php>.
- [73] G. Bertuccio et al, "New electrode geometry and potential distribution for X-ray drift detectors," *Nucl. Instr. and Meth. A*, vol. 312, no. 3, pp. 613-616, 1992.
- [74] J. Kemmer et al, "Low capacity drift diode," *Nucl. Instr. and Meth. A*, vol. 253, no. 3, pp. 378-381, 1987.
- [75] P. Lechner et al, "Silicon drift detectors for high resolution room temperature X-ray spectroscopy," *Nucl. Instr. and Meth. A*, vol. 377, no. 2-3, pp. 346-351, 1996.
- [76] R. Hartmann et al., "Ultrathin entrance windows for silicon drift detectors," *Nucl. Instr. and Meth. A*, vol. 387, no. 1-2, pp. 250-254, 1997.
- [77] D. M. Schlosser et al., "Expanding the detection efficiency of silicon drift detectors," *Nucl. Instr. and Meth. A*, vol. 624, no. 2, pp. 270-276, 2010.